

Charge Transfer and Electron-Correlation Effects in Alkali-Doped C₆₀

A. GUTIÉRREZ, S. L. MOLODTSOV† and G. KAINDL

Institut für Experimentalphysik, Freie Universität Berlin, Arnimallee 14, D-14195 Berlin-Dahlem, Germany.
† *On leave from Institute of Physics, St. Petersburg State University, 198904 St. Petersburg, Russia*

C. CASADO, M. E. DÁVILA, J. AVILA and M. C. ASENSIO

*Instituto de Ciencia de Materiales de Madrid, CSIC, C/Serrano 144, 28006 Madrid, Spain and L.U.R.E.,
Université Paris Sud F-91405 Orsay Cedex, France*

and

F. SORIA

Instituto de Ciencia de Materiales de Madrid, CSIC, C/Serrano 144, 28006 Madrid, Spain

The electronic structure close to the Fermi level of alkali-doped C₆₀ has been studied by photoemission (PE), resonant PE, and X-ray absorption spectroscopy (XAS). The results reveal a complete charge transfer from alkali atoms to fullerene and support a view where low-level-doped C₆₀ is considered a strongly correlated system.

1. Introduction

Despite the large number of experimental and theoretical studies^{1–6} of alkali-doped C₆₀, A_xC₆₀, a consistent interpretation of the electronic structure of these novel materials in the region close to the Fermi level (E_F) is still missing. Such an understanding of the electronic structure would be of particular interest for the superconducting phases K₃C₆₀ and Rb₃C₆₀. According to theoretical findings,^{4,5} the alkali atom transfers its valence electron to the fullerene, filling up, with increasing alkali content, the lowest unoccupied molecular orbital (LUMO) of C₆₀. However, as shown by spectroscopic studies, such a simple model is not completely correct.^{3,7} Photoemission (PE) studies show that the half-occupied LUMO-derived band in the superconducting phase A₃C₆₀ is even broader than the LUMO states are in pure C₆₀.^{2,8} In addition, the A₄C₆₀ phase seems to be an insulator.³

Recent studies^{2,9} have revealed an additional structure in the energy region close to E_F for very low alkali concentrations that can hardly be explained within the framework of single-particle band models. The results of Lof *et al.*¹⁰ gave evidence that undoped C₆₀ and probably also K₃C₆₀ has to be regarded as a correlated electron systems. Other authors^{2,11} demonstrated the importance of Hubbard-like band splittings in K₄C₆₀ and Rb₄C₆₀ as well as in Li₂C₆₀ and Na₂C₆₀.

The present study addresses some of these questions on the basis of valence-band and core-level PE, resonant PE, and X-ray absorption spectroscopy (XAS) studies of K-, Rb-, and Cs-doped fullerenes.

2. Experimental

The high-resolution PE measurements over a wide range of photon energies as well as the XAS measurements were performed using the SX700/II, TGM-6, and 3m-NIM-1 beamlines of the Berliner Elektronenspeicherring für Synchrotronstrahlung (BESSY), as well as the SU-6 undulator beamline of the Super-ACO storage ring in Orsay. An angle-integrating hemispherical electron-energy analyzer was used in the experiments at the SX700/II and 3m-NIM-1 beamlines, and rotatable hemispherical analyzers (VSW-ARIES) at the TGM-6 and SU-6 beamlines. The PE spectra were taken in normal emission geometry with a total-system resolution of 40 meV (FWHM) in the angle-integrated mode, and of 200 meV in the angle-resolved mode. XAS spectra were recorded in the total-electron-yield mode with a resolution of 100 meV (FWHM). The process of *in situ* sample preparation used in the present work has been described elsewhere.¹² Dopant levels were estimated by direct comparison of the relative PE intensities of signals from the highest occupied molecular orbital (HOMO) and the LUMO-derived state of A_xC_{60} with those of A_6C_{60} , the latter serving as reference compound with the highest possible alkali content. In addition, measurements of the electrical resistivity of the doped films were performed. These two methods, being surface and bulk sensitive, respectively, gave similar results reflecting the homogeneity of the prepared samples.

3. Results and discussion

A valence-band PE spectrum of a solid C_{60} film (thickness $\theta \simeq 80 \text{ \AA}$), taken at a photon energy of 35 eV, is shown in Figure 1. The spectrum has a similar shape and contains all features of the valence-band PE spectra reported previously. With our high-quality solid C_{60} films, however, we were able to resolve clearly a fine doublet structure with a high-binding-energy shoulder (features A, B, and C) that was only barely noticed in previous PE studies. The double structure could be observed for several different C_{60} films, but it was mostly prominent for photon energies around 35 eV. Since we do not expect appreciable changes in the photoionization cross section for states with nearly the same symmetry, the presence of the doublet can be caused by final-state effects, e.g. due to parity conservation rules,¹³ or by some kind of resonance involving both initial and final states.

The preparation process of solid films of A_xC_{60} was monitored by valence-band PE and C-1s XAS, as shown in Figure 2 for K_xC_{60} . In the XAS spectra, the absolute energy relative to E_F was determined by assuming the Fermi level to cross the LUMO-derived band in case of K_3C_{60} . Least-squares fit analysis (not shown in the figure) shows that the integrated intensity of the occupied LUMO states in the center spectrum of Figure 2 is about 3 times smaller than that of the HOMO states. While the spectra for undoped and fully-doped C_{60} are in agreement with insulating behavior, K_3C_{60} shows electronic states directly at E_F . These states form an asymmetric PE peak at E_F , intersected by the Fermi distribution function.

The PE spectrum of the half-doped K_3C_{60} film reveals a much broader structure, including the LUMO-derived band, that predicted by one-electron band theory.¹² This can result from energy losses of the photoelectrons¹⁴ or from correlation effects.¹¹ On the other hand, the formation of K_xC_{60} can lead to a rearrangement or hybridization of K- and C-derived states at the Fermi level in K_3C_{60} , different from what is expected in a simple charge-transfer model.

We also employed resonant PE at the $K 2p_{1/2} \rightarrow 3d$ absorption threshold in order to

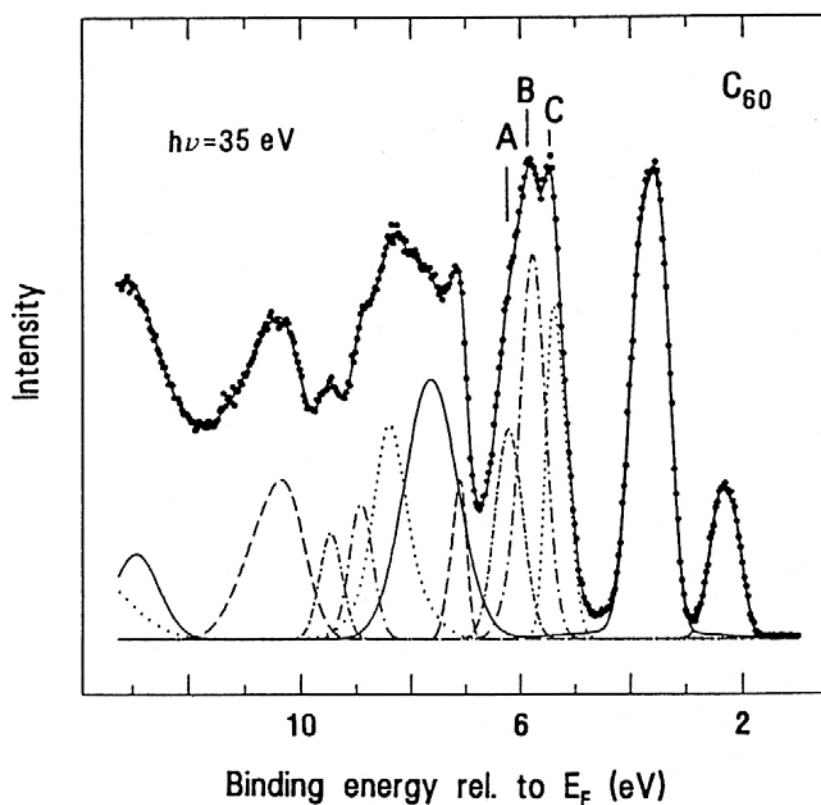


Figure 1 Valence-band PE spectrum of C_{60} for $h\nu = 35$ eV. A splitting of the HOMO+2 structure in three peaks (A, B, and C) is clearly observed.

obtain information on the partial K-derived electronic states close to E_F .¹² The resulting K $2p_{1/2} \rightarrow 3d$ on-resonance PE spectrum in the region of the HOMO and HOMO+1 states as well as the band located at a binding energy of $\simeq 5.7$ eV (HOMO+2), taken at a photon energy of 299.7 eV, is given in the inset of Figure 3 (spectrum (a)). The inset also shows an off-resonance spectrum taken at $h\nu = 245$ eV (spectrum (b)). The pure resonantly enhanced PE signal was obtained by subtracting the off-resonance spectrum from the on-resonance one. The result is shown in Figure 3 (top spectrum), where — for comparison — also the calculated K-p and K-d partial densities of states are plotted.¹² The calculated K-s partial density of states is negligible in this energy region as compared to K-p and K-d; in addition, it can hardly be observed with resonant PE due to its itinerant character. Both the experimental difference curve and the calculated partial density of states provide no evidence for the existence of K-derived states close to E_F , at binding energies up to $\simeq 1.5$ eV below E_F . These findings support a model of superconductivity in the alkali doped C_{60} ¹⁵ that is based on the pairing of alkali-transferred electrons at E_F via high-energy intramolecular phonons in C_{60} .

A coincidence in energies of the calculated p/d-hybridized states with the peaks in the resonantly enhanced PE spectrum, particularly in the binding energy region from $\simeq 1.5$ eV to 5.5 eV, reveals the origin of the PE resonance in K_3C_{60} . The overlap of K-p/d hybridized states with C-derived states can give rise to a broadening of the valence-band PE structures in the region of the HOMO, HOMO+1, and HOMO+2 bands. The same argument, however, cannot be applied to explain the broadening of the LUMO states, since no K-p/d states are found within 1.5 eV of the Fermi level. Therefore, correlation effects or electron-energy loss processes are more likely to cause the observed broadening of the LUMO-derived feature in the spectra of A_xC_{60} .

Since correlation effects are expected to be more pronounced in narrow band materials,

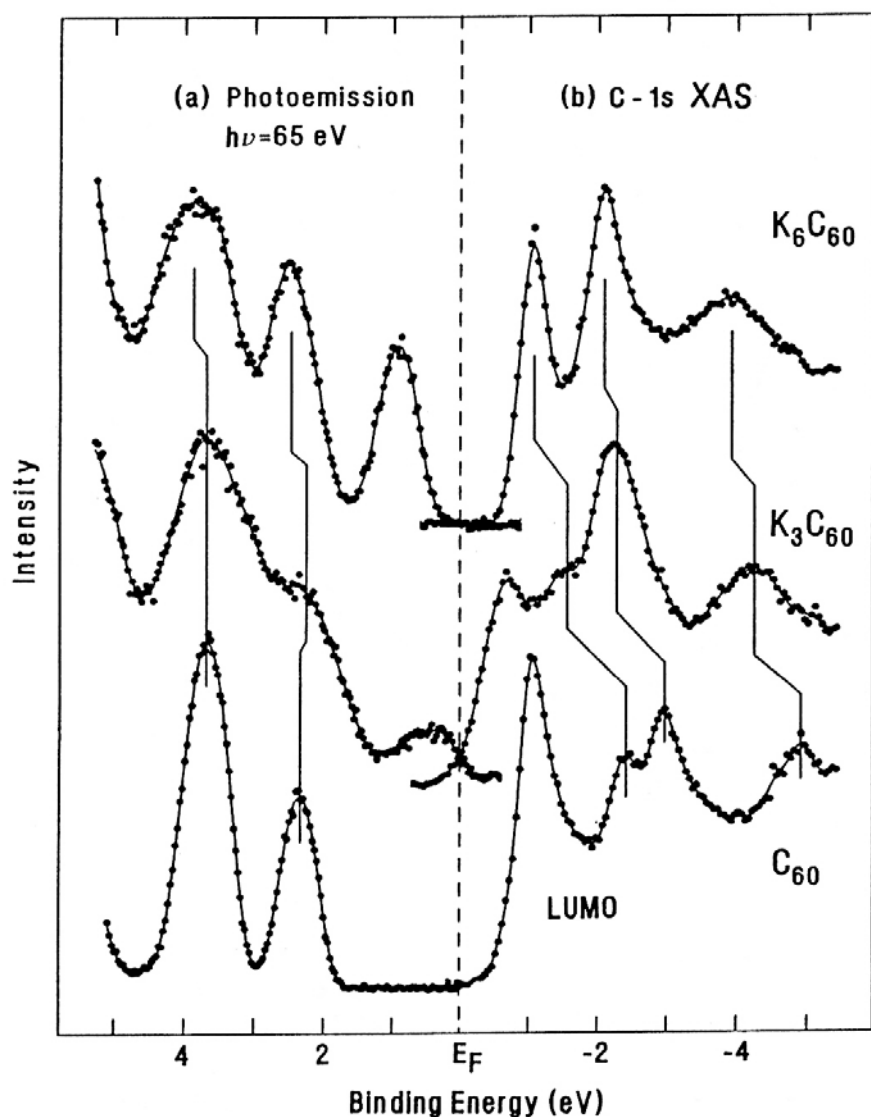


Figure 2 (a) Valence-band PE spectra of solid films of C_{60} , K_3C_{60} , and K_6C_{60} . (b) XAS spectra at the C-1s threshold taken in total-electron-yield mode.

we investigated changes in the electronic structure of K-, Rb-, and Cs-doped fullerites beginning with rather low levels of alkali concentrations. Figure 4 shows valence-band PE spectra of C_{60} films doped with K, recorded at $h\nu = 22$ eV. Similar sets of valence-band PE spectra were recorded for C_{60} films doped with Rb and Cs. For comparison, the PE spectrum of gas-phase C_{60}^- ions¹⁶ is also given by the solid line in the center of the figure. The energy scale of the gas-phase spectrum was positioned by aligning its HOMO with that of the $K_{1.7}C_{60}$ spectrum. For low doping concentrations, $x < 2.5$, a doublet structure with peaks A and B, located at BEs of ≈ 1.0 eV and ≈ 0.4 eV, respectively, is observed. With increasing x , the relative weight of peak A grows up to $x \approx 0.8$ and then decreases again. On the other hand, the relative weight of peak B increases gradually in such a way that the total intensity of features A and B scales linearly with the doping level.

Previously, similar effects have been observed for K-doped C_{60} ¹ and Li-doped as well as Na-doped C_{60} .² No indications for these phenomena, however, were found in the PE spectra taken at $h\nu = 65$ eV of C_{60} doped with K¹ and Rb.² In contrast to these observations, Takahashi *et al.*,⁹ employing low photon energies of 20 eV, have also found a double-peaked PE structure close to E_F for very low Rb concentrations in C_{60} . More recent PE studies, performed with a He resonance lamp,^{11,14} gave similar results for K-doped

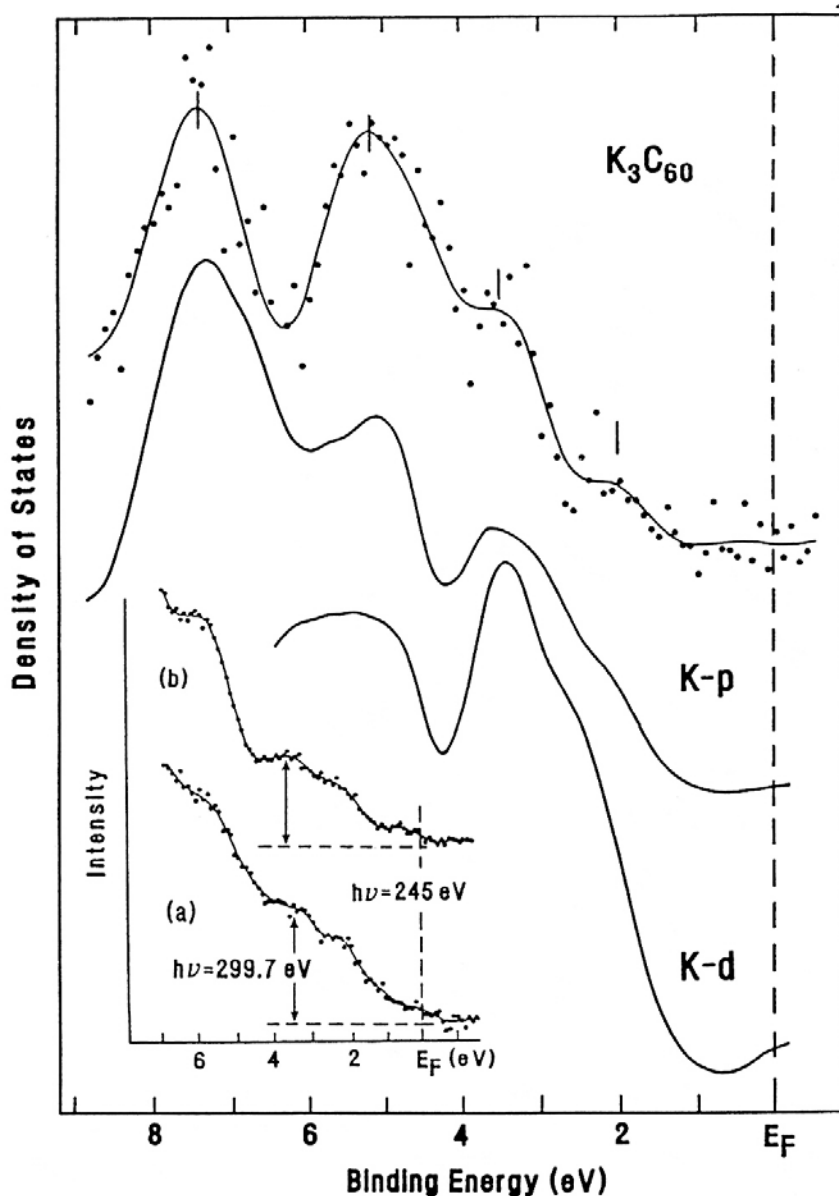


Figure 3 Comparison of the net resonantly enhanced PE signal at the K $2p_{1/2} \rightarrow 3d$ threshold with theoretical results for the K-p and K-d partial density of states of K_3C_{60} . The inset shows (a) the on-resonance and (b) the off-resonance PE spectra used to derive the net resonantly enhanced PE signal.

solid C_{60} .

According to Benning *et al.*,¹ an exposure of C_{60} to K at room temperature produces a dilute solid solution, $\alpha-C_{60}$. Phase separation into $\alpha-C_{60}$ and K_3C_{60} occurs if the K concentration exceeds the solubility limit. In contrast to the low-binding-energy feature B, peak A can hardly be assigned to the K_3C_{60} phase.^{11,14} On the other hand, the assumption that A stems from the $\alpha-C_{60}$ phase is supported by direct comparison of the spectrum of $K_{1.7}C_{60}$ with the one reported for single-ionized fullerene ions in the gas phase (see Figure 4).¹⁶

By exposing A_xC_{60} films to oxygen, we found a further argument to assign feature A to the dilute solid solution of alkali atoms in solid C_{60} . PE spectra of $Cs_{2.1}C_{60}$ before and after exposure to O_2 are shown in Figure 5(a). Independent of the initial alkali concentration, the signal in the energy region close to E_F (feature B) is quenched by low levels of oxygen dosing. At the same time, the intensity of structure A grows, reaching a value close to the intensity of the related feature for a doping level around $x \simeq 0.8$. Similar effects have

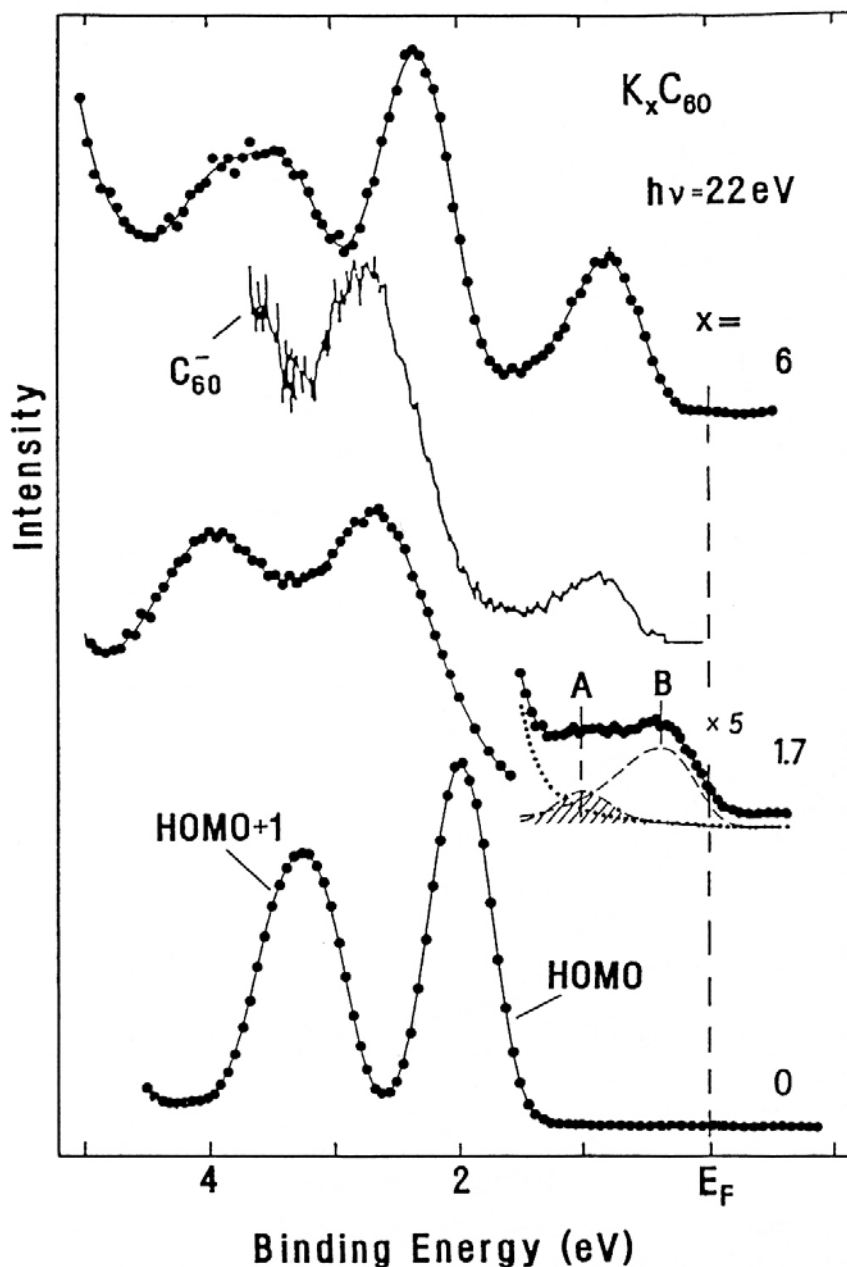


Figure 4 Valence-band PE spectra of $K_x C_{60}$ for various doping concentrations, x , together with the results of least-squares fit analyses of structure A (hatched component) and B (dashed line). The solid curve in the center represents the PE spectrum of C_{60}^- clusters in the gas phase, measured at $h\nu = 6.4$ eV.¹⁶

been observed for K- and Rb-doped C_{60} with various doping concentrations. A suspicion that feature A relates to the formation of alkali oxides can be ruled out, since much higher doses of O_2 exposure, which cause the growth of new structures originating from the alkali–O interaction (see inset in Figure 5),¹⁷ lead to a vanishing of structure A (arrow).

The oxidation of $K_x C_{60}$ leads to a depletion of K in the film in conjunction with a K–O reaction at the surface.¹ A deficiency of alkali atoms causes a depletion of occupied electronic states at E_F . As a result, only a small fraction of alkali atoms remains in the bulk of the C_{60} film forming a dilute solid solution, which is characterized by feature A in the PE spectrum. We investigated low-level doped C_{60} at various photon energies. The results are presented in Figure 6, revealing an increase in the intensity of the dash-dotted component for low photon energies, when the photoelectrons have a larger escape depth. This demonstrates the bulk origin of structure A.

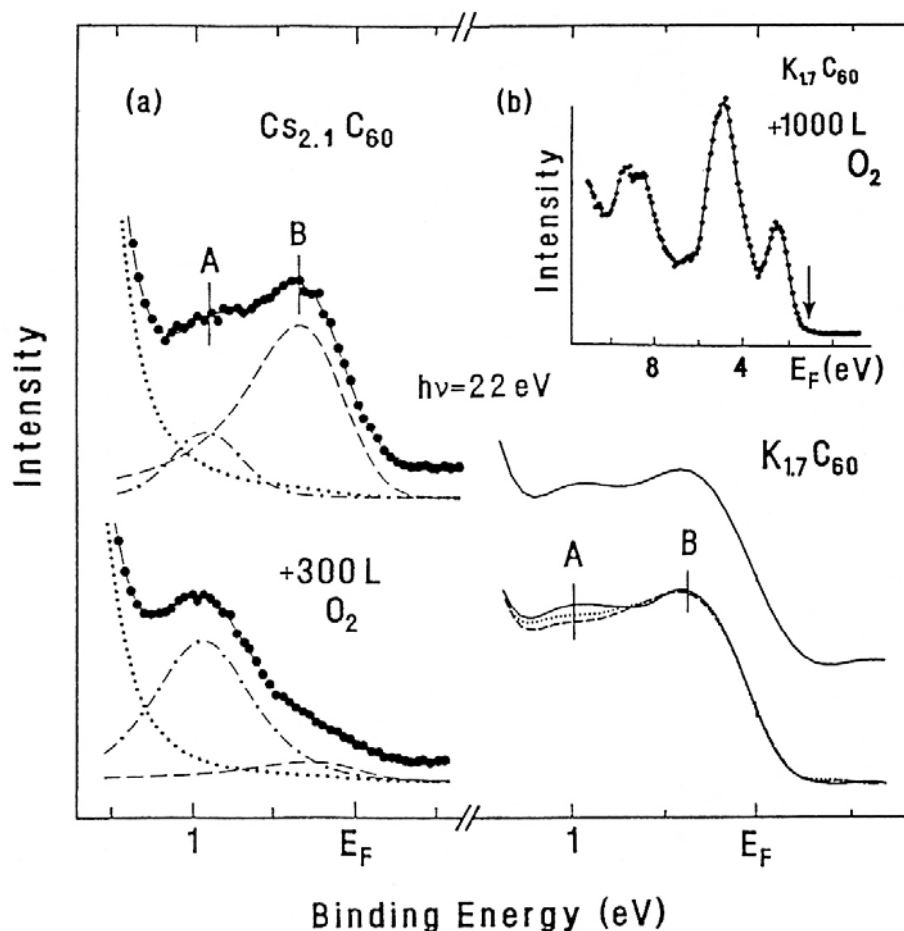


Figure 5 (a) PE spectra of $\text{Cs}_{2.1}\text{C}_{60}$ in the binding-energy region close to E_F taken from an as-grown film (top spectrum) and after exposure to 300 l of O_2 (bottom spectrum). (b) PE spectra of $\text{K}_{1.7}\text{C}_{60}$ taken from an as-grown film at room temperature (bottom spectrum, solid line) and after 10 min. (dotted line) and 15 min. (dashed line) annealing periods at 150°C , respectively. The corresponding spectrum obtained upon cooling the sample back to room temperature is shown in the upper solid line. The inset shows the PE spectrum of K-doped C_{60} after exposure to 1000 l of O_2 .

Recently, a reversible reaction, $\alpha\text{-C}_{60} + \text{K}_3\text{C}_{60} \leftrightarrow \text{KC}_{60}$, was observed for K_xC_{60} at elevated temperatures ($T \simeq 150^\circ\text{C}$).¹⁸ This process was also monitored in the present study by reversible spectral-shape changes when $\text{K}_{1.7}\text{C}_{60}$ was annealed at a temperature of 150°C for various periods of time (bottom curves in Figure 5(b)); the top spectrum in Figure 5(b) was recorded after the sample had cooled back to room temperature. The main differences are observed in the region of feature A, whose intensity decreases in the process of annealing (from solid curve to dashed curve), but returns upon cooling to room temperature.

An understanding of the structures in the valence-band PE spectra in the region close to E_F can be obtained on the basis of the results of theoretical studies,¹⁹ which claim an essential alkali-metal-induced distortion of C_{60} intramolecular bonds. As a result, one energy level splits upward from the five-fold-degenerate HOMO band. These changes may cause the experimental observations with respect to the electronic structure close to E_F of alkali-doped C_{60} . However, our observations rule out this possibility. First, the PE signal in feature A is more than 30 times weaker than the one from the HOMO-derived band, while according to Reference 19 the ratio should be 1/4. Second, the shift in energy of feature A relative to the HOMO band exceeds by far the theoretically obtained value of $\simeq 0.35$ eV. Our analysis shows that a different structure — the low-binding-energy shoulder H, split from the HOMO state by 0.55 eV (Figure 6) — relates directly to the

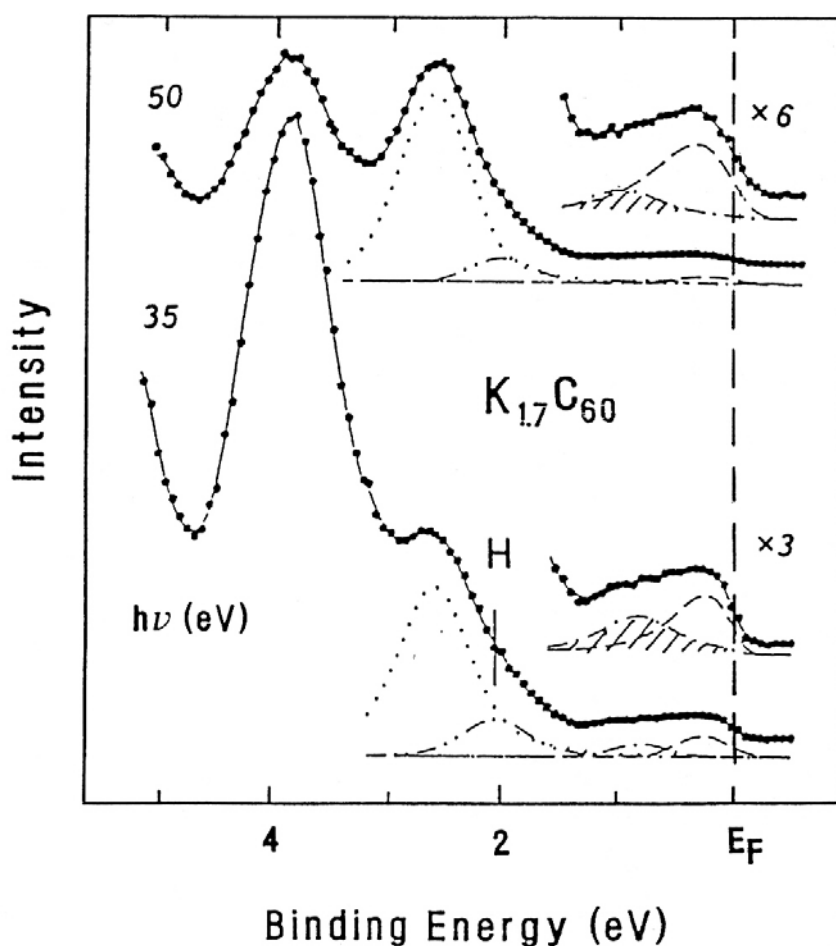


Figure 6 PE spectra of $K_{1.7}C_{60}$ taken at two photon energies, together with the results of least-squares fit analyses of the region close to E_F .

bond distortions caused by the reduced symmetry of C_{60} clusters in A_xC_{60} .

An alternative explanation is based on final-state effects in the photoionization process. The LUMO states with $p\pi^*$ symmetry are delocalized with respect to the molecule.⁸ On the other hand, the weak intermolecular van der Waals interactions in solid C_{60} cause the electron in these states to be confined to one particular position, resulting in a small hopping probability between neighboring molecules. For alkali concentrations higher than A_1C_{60} , there is at least one electron left in the LUMO state, which can screen the hole created in the PE process, giving rise to feature B. However, for lower alkali concentrations, there are no electrons left in the LUMO state, and consequently no local screening of the hole can occur. This results in a shift of the PE signal to higher binding energies, corresponding to feature A. This interpretation is supported by the PE spectrum of C_{60}^- in the gas phase, where the PE LUMO final state cannot be screened, resulting in a shift of the LUMO-derived peak to higher binding energies (see Figure 4). The coexistence of phases with different concentrations in K_xC_{60} for $0 < x < 3$ would account for the double structure observed in Figures 4–6.

Acknowledgements

S.L.M. thanks the Alexander von Humboldt-Stiftung for financial support and the Freie Universität Berlin for hospitality. A.G. acknowledges financial support by the Spanish Ministerio de Educación y Ciencia. Fruitful discussions with C. Laubschat and E. Navas are gratefully acknowledged. This work was supported by the Bundesminister für Forschung

und Technologie, project No. 05-5KEAXI3/TP01, the Deutsche Forschungsgemeinschaft, Sonderforschungsbereich-290, TPA06, the Beamline-Installation Program of L.U.R.E., and the project of the Comisión Interministerial de Ciencia y Tecnología MAT 92-0937.

References

1. P. J. Benning, D. M. Poirier, T. R. Ohno, Y. Chen, M. B. Jost, F. Stepniak, G. H. Kroll, J. H. Weaver, J. Fure, and R. E. Smalley. *Phys. Rev. B*, **45**, 6899 (1992).
2. C. Gu, F. Stepniak, D. M. Poirier, M. B. Jost, P. J. Benning, Y. Chen, T. R. Ohno, J. L. Martins, J. H. Weaver, J. Fure, and R. E. Smalley. *Phys. Rev. B*, **45**, 6348 (1992).
3. M. Merkel, M. Knupfer, M. S. Golden, J. Fink, R. Seemann, and R. L. Johnson. *Phys. Rev. B*, **47**, 11470 (1993).
4. J. L. Martins and N. Troullier. *Phys. Rev. B*, **46**, 1766 (1992).
5. S. Satpathy, V. P. Antropov, O. K. Andersen, O. Jepsen, O. Gunnarsson, and A. I. Liechtenstein. *Phys. Rev. B*, **46**, 1773 (1992).
6. M. Z. Huang, Y. N. Xu, and W. Y. Ching. *J. Chem. Phys.*, **96**, 1648 (1992).
7. G. K. Wertheim and D. N. E. Buchanan. *Phys. Rev. B*, **47**, 12912 (1993).
8. S. L. Molodtsov, A. Gutiérrez, M. Domke, and G. Kaindl. *Europhys. Lett.*, **19**, 369 (1992).
9. T. Takahashi, T. Morikawa, S. Sat, H. Katayama-Yoshida, A. Yuyama, K. Seki, H. Fujimoto, S. Hino, S. Hasegawa, K. Kamiya, H. Inokuchi, K. Kikuchi, S. Suzuki, K. Ikemoto, and Y. Achiba. *Physica C*, **185-189**, 417 (1991).
10. R. W. Lof, M. A. van Veenendaal, B. Koopmans, H. T. Jonkman, and G. A. Sawatzky. *Phys. Rev. Lett.*, **68**, 3924 (1992).
11. P. J. Benning, F. Stepniak, D. M. Poirier, J. L. Martins, J. H. Weaver, L. P. F. Chibante, and R. E. Smalley. *Phys. Rev. B*, **47**, 13843 (1993).
12. S. L. Molodtsov, A. Gutiérrez, E. Navas, M. Domke, G. Kaindl, M. Merkel, N. Nücker, J. Fink, V. P. Antropov, O. K. Andersen, and O. Jepsen. *Z. Phys. B*, **92**, 347 (1993).
13. P. J. Benning, D. M. Poirier, N. Troullier, J. L. Martins, J. H. Weaver, R. E. Haufler, L. P. F. Chibante, and R. E. Smalley. *Phys. Rev. B*, **44**, 1962 (1991).
14. M. Knupfer, M. Merkel, M. S. Golden, J. Fink, O. Gunnarsson, and V. P. Antropov. *Phys. Rev. B*, **47**, 13944 (1993).
15. M. Schluter, M. Lannoo, M. Needels, G. A. Baraff, and D. Tomanek. *Phys. Rev. Lett.*, **68**, 526 (1992).
16. S. H. Yang, C. L. Pettiette, J. Conceicao, O. Cheshnovsky, and R. E. Smalley. *Chem. Phys. Lett.*, **139**, 233 (1987).
17. J. Jupille, P. Dolle, and M. Besancon. *Surf. Sci.*, **260**, 271 (1992).
18. D. M. Poirier and J. H. Weaver. *Phys. Rev. B*, **47**, 10959 (1993).
19. K. Harigaya. *Phys. Rev. B*, **45**, 13676 (1992).